Powder Technology 229 (2012) 24–29

Contents lists available at SciVerse ScienceDirect

Powder Technology

journal homepage: www.elsevier.com/locate/powtec

Electrochemical characteristics of cathode materials NiS_2 and Fe-doped NiS_2 synthesized by mechanical alloying for lithium-ion batteries

X.J. Liu [a], Z.Z. Xu [b], H.J. Ahn [a], S.K. Lyu [b], I.S. Ahn [a,*]

[a] School of Material Science & Engineering, Gyeongsang National University, Jinju 660-701, South Korea
[b] School of Mechanical & Aerospace Engineering, Gyeongsang National University, Jinju 660-701, South Korea

ARTICLE INFO

Article history:
Received 21 October 2011
Received in revised form 21 February 2012
Accepted 13 May 2012
Available online 19 May 2012

Keywords:
Mechanical alloying
Lithium-ion batteries
Wet milling
Nickel disulfide and Fe-doped nickel disulfide cathodes

ABSTRACT

In this study, fine cathode materials NiS_2 and Fe-doped NiS_2 are prepared by mechanical alloying (MA), small mean particle sizes of each other are obtained through wet ball-milling. To compare the performance of Li/NiS_2 and Li/Fe-doped NiS_2 cells prepared by both Planetary Ball Mill (PBM) and SPEX Mill (SM) respectively, the following results have been revealed: SM can do a great deal towards improving the initial discharge capacity of both cells; the cycle life of all cells prepared by PBM was better than SM which is may be due to the small number of lattice defects and low internal stress for different milling conditions used; wet milling process can help to improve the whole characteristic of Li/Fe-doped NiS_2 cells, but not seem to apply to Li/NiS_2 one; the main factor influencing the performance of Li-ion cells is the doping of iron elements, which may stable the crystal structure in the process of intercalation and deintercalation of lithium ions between the active materials.

1. Introduction

With the increasing popularity of portable electronic products such as cellular phones, laptops, camcorders and the pressing need for high specific energy storage in aviation, aerospace, electric vehicles and other high-tech fields, lithium-ion batteries came into being as one source of high specific energy, and were widely applied in industries. However, due to the shortcomings of existing practical commercial cathode materials such as $LiCoO_2$, $LiMn_2O_4$ and $LiNiO_2$, (which have been greatly limited in some ranges due to poor cobalt resources, bad electrochemical performance at high temperature and horrible problems in the manufacture process, respectively [1]), the development of new battery systems, especially for research and development of new electrode materials and better electrolytes, is becoming extremely urgent.

According to the 3E principle proposed by P. Rüetschi [2], of Energy, Economics and Environment, metal disulfides have been hailed as one of the most promising cathode materials as they are cheap, non-toxic, available in abundance and can provide high energy density. Therefore, much investigation on methods to synthesize metal disulfides (FeS_2, NiS_2 etc.) has been done, from the traditional method of reacting stoichiometric amounts of their constituent elements in evacuated silica tubes at high temperature (1000–1200 °C) [3] to a solid-state reaction between potassium hexafluoro-nickelate (IV) and sodium pentasulfide hydrate at ~65 °C [4], from precursor-synthesization [5] to low-temperature solvent-thermal synthesization [6,7] either due to their fundamental importance as magnetic materials [8], photoactive materials [9] or solid-state lubricants [10] or their rosy prospects for application in portable devices and even for EVs and HEVs. However, it is difficult to control the manufacturing process, not only due to the high temperatures required or the pollution it creates, but also the related high costs and complexity.

In this study, we will prepare fine compounds of NiS_2 and Fe-doped NiS_2 using a new, simple, effective and convenient process, mechanical alloying, which has not received much attention in the field of lithium batteries (until Disma's [11] early study on raising the electroactivity of lithium through a milling process), yet can provide a way for direct solid-state synthesis and help to improve the purity of the resultant substances. In addition, the wet milling process was conducted with the aim of decreasing particle size to cut down the diffusion path of lithium-ions between the active materials and further improve the charge/discharge capacity while optimizing cycle life. Finally, comparisons between NiS_2 and Fe-doped NiS_2, including synthesis, charge/discharge capacities, cycle life and so on, focus on assessing their comprehensive performance and further deciding which is the superior cathode material.

2. Experimental procedures

2.1. Dry milling process

In order to compare the charge/discharge properties and cycle life of Li/NiS_2 and Li/Fe-doped NiS_2 cells, stoichiometric amounts of metal and sulfur powders (99.5%, −100 mesh) were prepared according to

* Corresponding author. Tel.: +82 55 772 1662; fax: +82 55 772 1670.
E-mail address: ais@gnu.ac.kr (IS. Ahn).

0032-5910/$ – see front matter © 2012 Elsevier B.V. All rights reserved.
doi:10.1016/j.powtec.2012.05.035

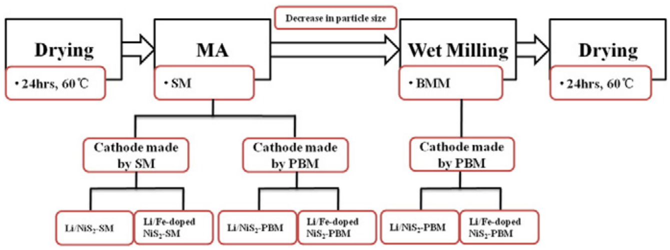

Fig. 1. Flow chart of NiS_2 and Fe-doped NiS_2 compound preparation and schematic diagram of the cell tests, in which cathodes were prepared using different active materials and different grinding machines.

1:2, for NiS_2, the metal powder was nickel (99.9%, <10 μm) only, but in the case of Fe-doped NiS_2, the metal powders also included iron (99.9%, <10 μm) particles, and their atomic ratio was set as 9:1. In addition, an appropriate quantity of stearic acid ($CH_3(CH_2)16CO_2H$) was added as a kind of process control agent (PCA) to prevent excessive cold welding and severe agglomeration from occurring in the process of mechanical alloying. Same-type 5 mm stainless steel balls were used, and the ball powder ratio were kept constant at 30: 1 and 20: 1, respectively. All mixture handling (loading and un-loading) were done in an argon-filled glove box to avoid oxidation. In the final step, NiS_2 and Fe-doped NiS_2 fine compounds were obtained after 4 h and 4.5 h milling, respectively, with an SPEX Mill (SM) at a high speed of 1000 rpm.

2.2. Wet milling process

As is known, the smaller the particle size, the larger the contact areas between the active materials, the shorter the diffusion path of Li-ions and the better the cycle life. In this study, about 3 g alloyed NiS_2 and Fe-doped NiS_2 powders were loaded into the milling jar respectively with normal hexane (C_6H_{14}) which occupied 70% of the jar volume, with several stainless steel balls of 5 mm and 9.5 mm (weight ratio was 1:1). Here, wet milling process was conducted under the same conditions including constant BPR of 150:1, milling time of 30 h and milling speed of 300 rpm. The resulting powders were both filtered and dried for 24 h at 60 °C in a vacuum drying oven.

2.3. Preparation of cathodes and electrolytes

To prepare NiS_2 and Fe-doped NiS_2 cathodes, the active materials (NiS_2 powders, or Fe-doped NiS_2 powders, 60 wt.%) were separately mixed with PEO (polyethylene oxide, 20 wt.%), Super-P (MMM Carbon, 20 wt.%) and ACN (acrylonitrile) uniformly to prepare slurries which were coated on aluminum foil at room temperature using the doctor-blade casting method. In addition, with the aim of studying the electrochemical properties of Li/NiS_2 and Li/Fe-doped NiS_2 cells, the relative cathodes were prepared by both SM and PBM at a speed of 1000 rpm for 2 h and 300 rpm for 3 h respectively. The prepared films were dried at 80 °C for 24 h in an air oven and then cut into disk electrons (1.1 cm diameter) and stored within an argon-filled glove box. Meanwhile, the cathodes using wet milled powders were also prepared in the above-mentioned way by PBM, and the same electrolyte was used for all tests by dissolving 1 M $LiCF_3SO_3$ (Aldrich Chem. Co.) salt into TEGDME (Aldrich Chem. Co.). The whole schematic diagram of the milling order is described and shown in Fig. 1 to aid understanding of the experiment.

2.4. Assessment and measurement

In this study, a field emission scanning electronic microscope (FE-SEM) was used to investigate the surface morphologies of the powder particles, and X-ray diffraction (XRD) was conducted to examine the crystal structure and composition of synthesized compounds, on which the experimental diffraction patterns were collected with a scanning step of 0.02° at a range of $10° < 2\theta < 90°$ using a graphite monochromator. In addition, an energy-dispersive X-ray spectrometer (EDS) was used to perform chemical analysis in the FE-SEM and map the surface image of the alloyed powders. HELOS Particle Size Analysis was used to measure the mean particle size of mechanical alloyed compounds before and after the wet milling process. Moreover, transmission electron microscopy (TEM), with an analytical microscope operated at 200 kV, was employed to observe sample structures, and a WBCS 3000 Battery Tester (WonA Tech) was used to study the electrochemical properties of Li/NiS_2 and Li/Fe-doped NiS_2 cells at normal temperature.

3. Results and discussion

Fig. 2 shows micrographs of the starting elements used in this study. The spherical nickel and iron powders shown in Fig. 2 (a) and (b) both have a good size distribution with mean particle size of 7 and 5 μm respectively, while the images of soft sulfur and papery stearic acid powder particles are also severally shown in Fig. 2 (c) and (d).

In actuality, the dry ball milling process here is the mechanical alloying course, in which the powder particles were repeatedly flattened, cold welded, fractured and re-welded, resulting in the generation of a variety of crystal defects, such as dislocation, stacking faults, vacancies and so on. As the balance between cold welding and fracturing of the powder particles is responsible for the change in crystal structure and size distribution, we have researched the phase transformation (shown in Fig. 4) and taken images of the powder particles after different milling times, as shown in Fig. 3. Clearly we can see that the longer the milling time, the smaller the powder particles and the better the size distributions before nickel disulfide was formed, which can also indirectly indicate that during the alloying process the rate of fracturing is higher and tends to be balanced with cold welding by virtue of the lower rate of powder size reduction. Although NiS_2 and Fe-doped NiS_2 fine compounds were synthesized after 4 h and 4.5 h ball milling respectively, the ever-present phenomenon of agglomeration still could not be prevented, even if PCA had been added to prevent excessive cold welding. This is why

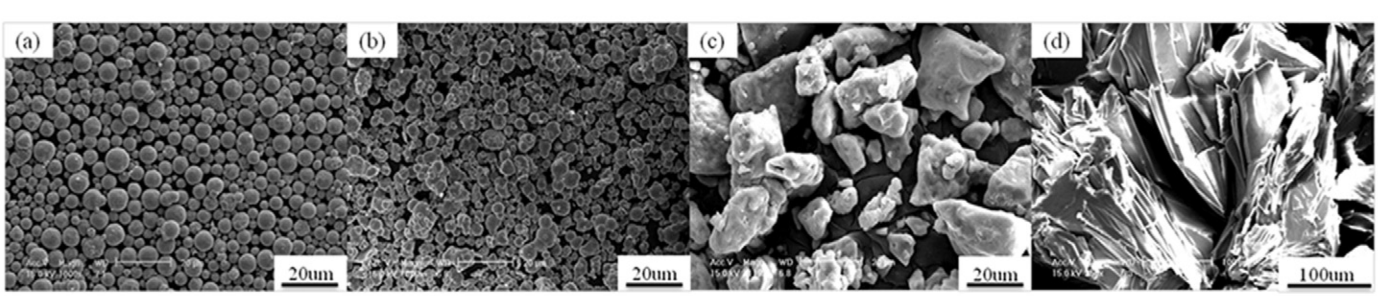

Fig. 2. FE-SEM micrographs of starting materials: (a) nickel, (b) iron, (c) sulfur and (d) stearic acid.

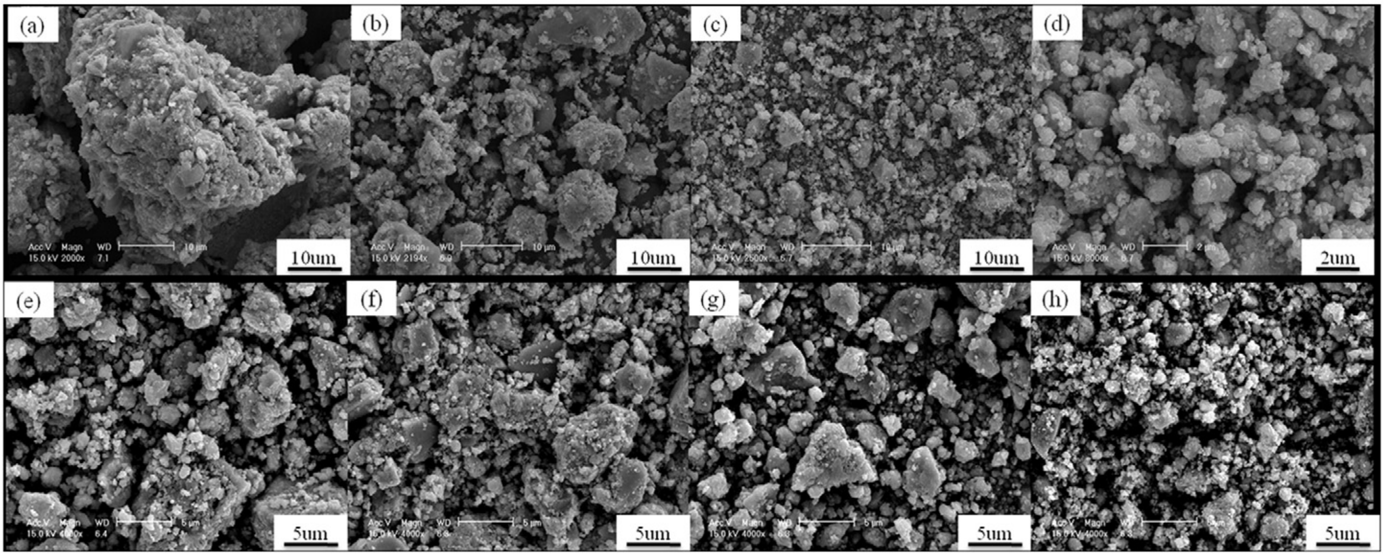

Fig. 3. FE-SEM micrographs of mechanically-alloyed powder particles in the dry milling process with different milling times. (a), (b), (c), and (d) are of the resultant powders after 1 h, 2 h, 3 h and 4 h of ball milling for the synthesis of NiS_2, while (e), (f), (g), and (h) are the resultant particles after 1.5 h, 2.5 h, 3.5 h and 4.5 h of ball milling for the synthesis of Fe-doped NiS_2.

we need to conduct the wet milling process next to make the test results better for both cells.

The phase transformation of NiS_2 (a) and Fe-doped NiS_2 (b) during the dry ball milling process was completely recorded and displayed by XRD patterns shown in Fig. 4, from which we can get the following information: after 2 h of ball milling, NiS_2 was formed little by consuming part of the starting materials of nickel and sulfur; after 3 h, most nickel disulfide peaks replaced the original positions of raw elements, which may indicate that powder mixtures subjected to heavy plastic deformation are activated to induce explosive reactions between the nickel and sulfur. In order to decrease the particle size, ball milling was continuous for a total of 4 h. Clearly, there was no new phase formed during this period, but the size distribution greatly improved, which can be certified in the FE-SEM micrographs shown in Fig. 3 (a). The synthesis of Fe-doped NiS_2 also went through the same course as NiS_2 and most of its peaks emerged after 4.5 h of ball milling. Here it should be noted that no iron peaks appeared after 2.5 h of ball milling, which may indicate that iron was successfully doped into the crystal structure of the NiS_2. After wet milling, both not only formed free of impurities in comparison with the dry ones, but the peaks were also broadened, indicating particle size had been greatly refined. Meanwhile, both patterns have a good agreement with the representative cubic NiS_2 phase (JCPDS card no. 85-1802) after the wet milling process. In addition, other important information can be also derived by virtue of the XRD patterns, from the perspective of residual stresses in an object, which are theoretically divided into these three kinds: micro-stress, macroscopic stress and ultra-microscopic stress. As we know, the uniform strain, produced by micro-stress that uniformly distributed in a wide range of objects, can lead to an aeolotropic displacement of the diffraction lines (variation of 2θ), while macroscopic stress in each grain or even various parts of one grain are so different that the uneven strain will make the diffraction lines diffuse and wide, also the ultra-microscopic stress in the strain region make the atoms deviate from their equilibrium position (resulting in lattice distortion) and further weaken the intensity of diffraction. Therefore, through Fig. 4 (a), we can see that for the same lattice plane, the longer the dry milling time is, the larger the variation of 2θ to standard, and the wider the diffraction peaks are, both indicating more and more micro-stress and macroscopic stress occurred in the milling process, and after wet milling process, the diffraction intensity depressed greatly due to their joint effect of generant smaller particles and the ultra-

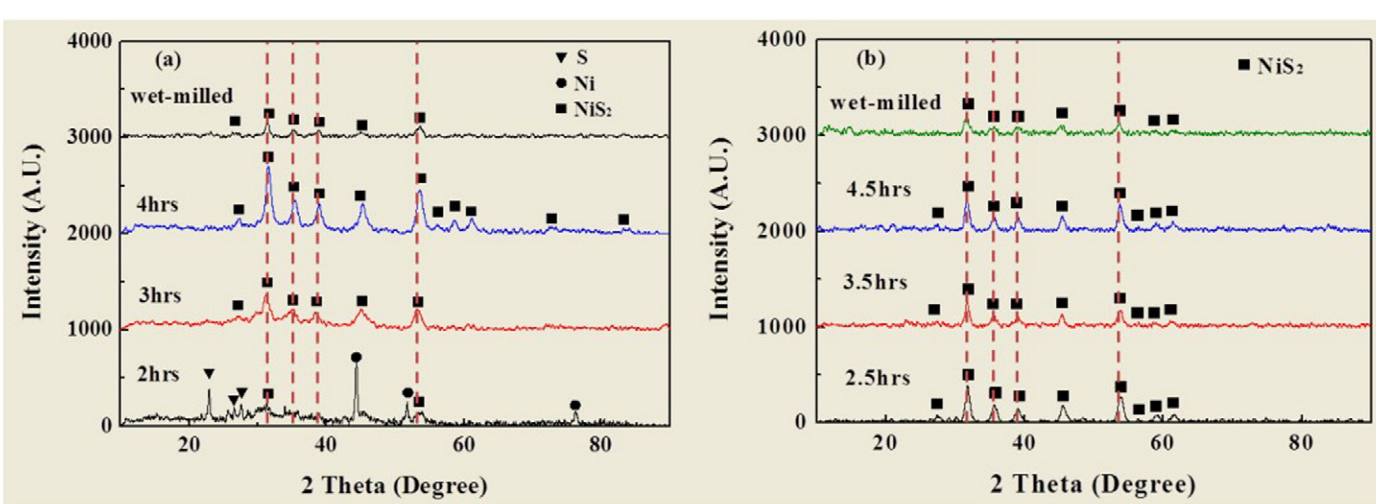

Fig. 4. XRD patterns of alloyed NiS_2 (a) and Fe-doped NiS_2 (b) powder particles before and after the wet ball milling process.

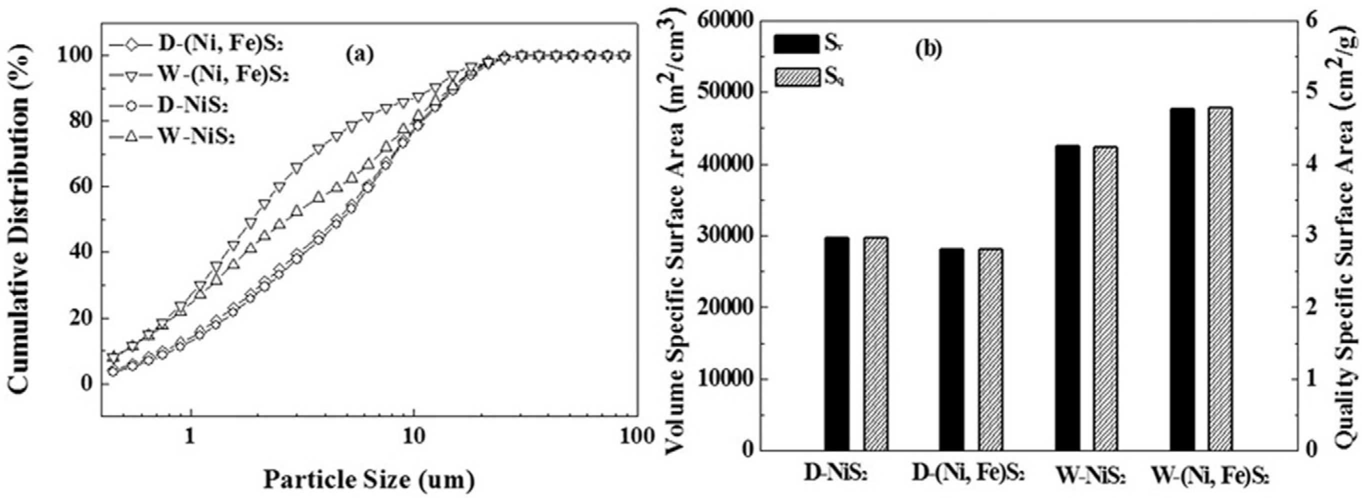

Fig. 5. Cumulative distribution curves (a), volume and quality-specific surface area (b) of NiS_2 and Fe-doped NiS_2 powders before and after wet milling process.

microscopic stress. Meanwhile, from Fig. 4 (b), bare of variation of 2θ to standard for the same crystal surface occurred as the milling time increased, however, the diffraction peaks seemed to be wide, which may be caused by the formation of macroscopic stress due to the doping of iron element.

Also, the cumulative distribution curves of NiS_2 and Fe-doped NiS_2 powders before and after the wet milling process were measured and are shown in Fig. 5 (a). The profiles of dry milled NiS_2 and Fe-doped NiS_2 powders are very similar to each other and the corresponding mean grain size of 4.71 and 4.50 μm can be tested separately. However, after wet grinding, particles were greatly decreased in size, especially in the Fe-doped NiS_2 powders for its cumulative distribution curve has always been at the top of all the others. As is known, the abscissa value of particle size corresponding to the ordinate value 50% of cumulative distribution is defined as mean particle size, so the particle sizes of NiS_2 and Fe-doped NiS_2 wet milled powders were 2.69 and 1.89 μm respectively. In addition, the volume- (S_v) and quality- (S_q) specific surface areas of both these powders before and after the wet grinding process were also tested and are shown in Fig. 5 (b). Obviously most conform to the common situation that the smaller the mean particle size, the higher the S_v and S_q, other than the dry milled NiS_2 powders (not only its mean size but also the S_v and S_q are both bigger than Fe-doped powders, which may indicate poor size or density distribution relative to the others).

Fig. 6 shows the FE-SEM micrographs and EDS mapping results of the wet milled NiS_2 (a) and Fe-doped NiS_2 (b) powder particles. Clearly, the elements of nickel and sulfur both have a good distribution on the surface of the nickel disulfide powders. In order to analyze the situation of iron doping, the atomic percent of the constituents has also been tested, and the results showed sulfur, nickel and iron elements were 65.72%, 34.16%, 0.12% and 63.11%, 32.33%, 4.56% respectively for NiS_2 and Fe-doped NiS_2 wet milled samples. According to the chemical formulation of nickel disulfide, the ratio of sulfur to nickel is a little smaller than the theoretical value, about 1.92 and 1.95 respectively, which may indicate the lack of sulfur as it is soft and can easily adhere to the interface of the milling jar in MA. Meanwhile, that the iron has been well doped in NiS_2 can be certified by its good distribution on the surfaces of the alloyed Fe-doped NiS_2 powders.

Fig. 7 shows the TEM micrographs and FE-SEM images of wet milled NiS_2 and Fe-doped NiS_2 powder particles. From Fig. 7 (a) and (c), we can get that nanocrystalline of NiS_2 and Fe-doped NiS_2 with an average size of 38 and 27 nm can be easily obtained after the wet milling process. However, for the features of nano powders, the

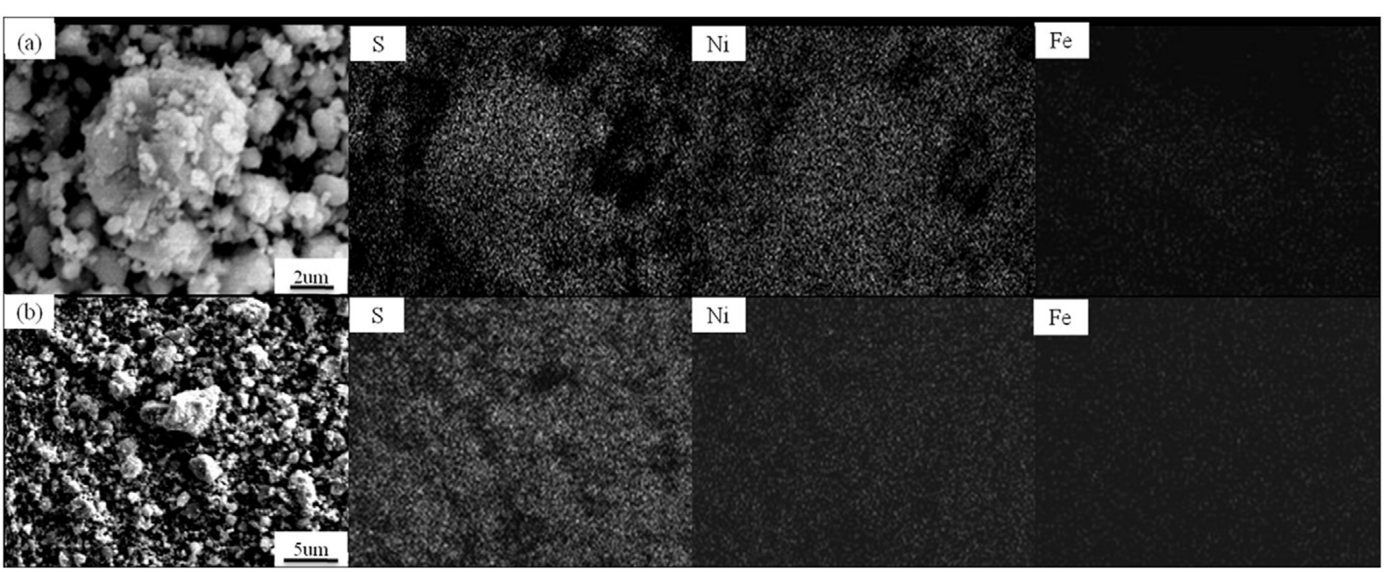

Fig. 6. FE-SEM micrographs and EDS mapping results of wet milled NiS_2 (a) and Fe-doped NiS_2 (b) particles.

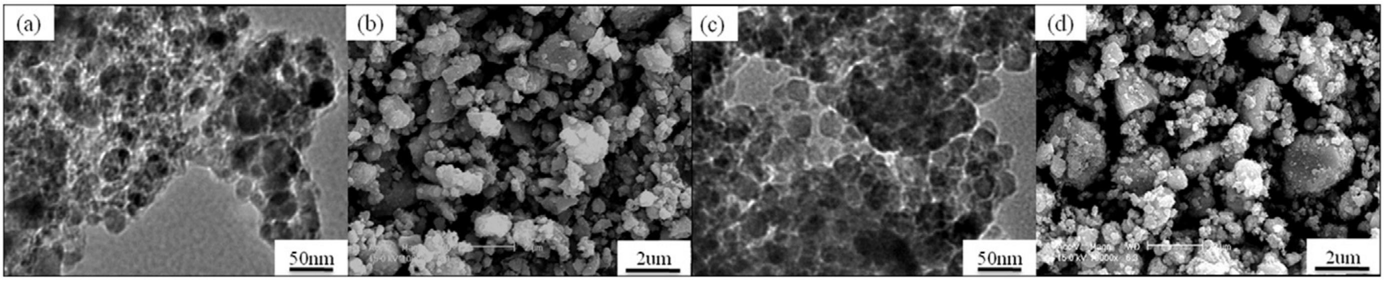

Fig. 7. TEM micrographs and FE-SEM images of NiS_2 (a, b) and Fe-doped NiS_2 (c, d) powder particles after the wet milling process.

phenomenon of agglomeration isn't inevitable, and this is clearly certified in Fig. 7 (b) and (d), even though the wet milling process was applied to disperse and separate the powder particles for 30 h. But when compared with dry production, particle size distribution can be seen to have greatly improved, and this may contribute to the thermal stability of both cells.

In this study, we held the voltage range (between 0.8 and 2.4 V), current density (0.1 C) and potential scan rate (0.1 mV s^{-1}) constant for all tests to eliminate the possibility that comparison errors will occur as a result of different parameters being set. In order to study the impact of different grinding machines on the electrochemical properties of Li-ion batteries, the initial discharge curves of Li/NiS_2 and Li/Fe-doped NiS_2 cells both prepared by PBM and SM using dry milled powder particles is shown in Fig. 8. Clearly, SM-NiS_2 displays the highest initial discharge capacity of 915 mAh g^{-1}, a little better than SM-Fe-doped NiS_2 (at 889 mAh g^{-1}), but far superior to the corresponding PBM-NiS_2 and PBM-Fe-doped NiS_2 provided with 676 and 607 mAh g^{-1} respectively. Because of this, it is worth noting that the use of SM can do a great deal towards increasing initial discharge capacity of the cells, as the high speed and good dispersibility of SM can greatly contribute to decreasing powder size, and improving the homogeneity of the mixture, which further increases the capacity of the first discharge.

The cycle performances of Li/NiS_2 and Li/Fe-doped NiS_2 cells prepared by both SM and PBM were investigated for up to 20 cycles at room temperature, and the results are given in Fig. 9. The SM-NiS_2 and SM-Fe-doped NiS_2 cells both have higher discharge capacities than the corresponding cells prepared by PBM in the first few cycles and then lowered. As is known, particle size distribution, internal stress and defects in crystal lattice, homogeneity of powders, adhesives and conductive materials, and flatness of the electrodes can all have great impact on cycle performance of Li-ion batteries, so here we can make a reasonable guess that the cells prepared by SM can have a higher discharge capacity due to their better size distribution and preferable homogeneity of all necessary additives (these may play a leading role in the first early cycles), with the extension of the cycle testing, the attenuation of discharge capacity increased rapidly, mainly for its higher internal stress mentioned before and defects in crystal lattice (it can greatly hindered the intercalation and deintercalation of lithium ions between the active materials). In addition, through comparison of Li/NiS_2 and Li/Fe-doped NiS_2 cells, we can see that no matter what kind of grinding machine is used, Fe-doped cells have good cycle characteristics on the whole, and this may be due to part of the iron atoms replacing some nickel atomic positions, stabilizing the nickel disulfide crystal structure and further slowing down recession of capacity. In other words, SM can help to increase the initial discharge capacity, but goes against the cycle characteristics, so in order to improve the overall cell performance, the electrodes were later all prepared by PBM to decrease internal stress and crystal lattice defects.

It has been widely reported that the smaller the particle size, the higher the specific surface area is, the bigger the reaction activation energy and the more easily the process of intercalation/deintercalation of Li^+ occurs [12,13]. To further demonstrate this effect, wet milling process was conducted to decrease the mean particle size of active materials, and further, Li/NiS_2 and Li/Fe-doped NiS_2 cells were prepared by SPM under the same conditions to compare their performance at room temperature, the initial charge/discharge capacities of both cells were also measured and shown in Fig. 10. The Fe-doped cell has an initial high discharge capacity of 938 mAh g^{-1} with a flat voltage plateau about 1.7 V, while the other cell provided with 608 mAh g^{-1} gave a relatively shorter stable region of 1.5 V,

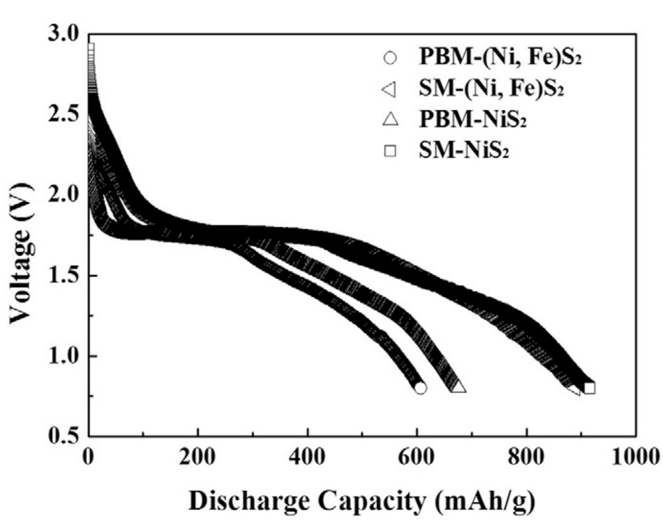

Fig. 8. Initial discharge curves of Li/NiS_2 and Li/Fe-doped NiS_2 cells prepared by both PBM and SM using dry milled powder particles at room temperature.

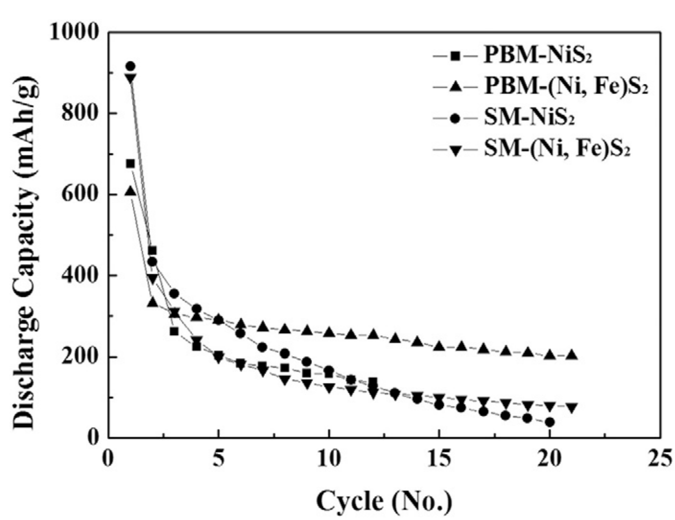

Fig. 9. Cycle performances of Li/NiS_2 and Li/Fe-doped NiS_2 cells prepared by both PBM and SM using dry milled particles at room temperature.

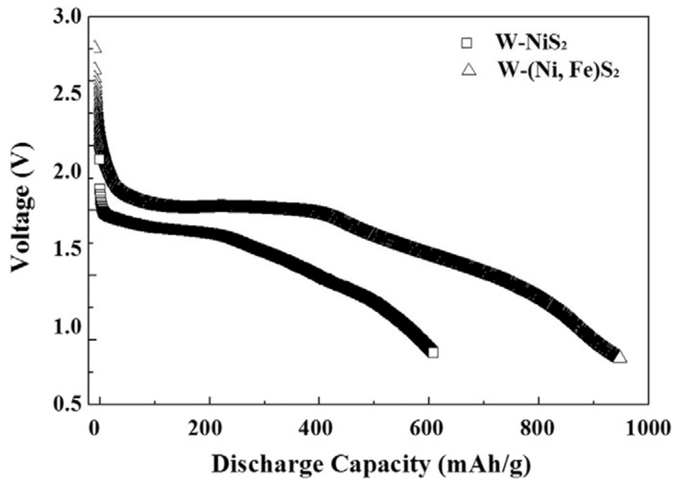

Fig. 10. Initial discharge curves of Li/NiS_2 and Li/Fe-doped NiS_2 cells prepared by PBM using wet milled powder particles at room temperature.

which may indicate that the doping of iron atoms into the NiS_2 crystals not only can decrease internal resistance to improve discharge voltage, but can also increase the first discharge capacity. However, the wet milling process seems to work poorly with nickel disulfide: not only was its first discharge capacity lower than with dry milling, but it also displayed a relatively short stable discharge region. The reason for this situation can be assumed as serious damage occurring to the crystal structure due to the lengthy ball milling, which can also increase the internal stress and further prevented the shuttle of Li-ions between the active materials as what we mentioned before.

In order to compare cycle properties between Li/NiS_2 and Li/Fe-doped NiS_2 cells using wet milled powder particles, the charge/discharge capacities versus cycle numbers have been tested under the same conditions as dry milled Li/NiS_2 and Li/Fe-doped NiS_2 cells, with results shown in Fig. 11. Clearly, the charge/discharge capacities of both cells faded with cycle numbers in almost the same pattern during the entire testing process. Also, for Fe-doped cells, it seems that the capacity recession phenomenon always exists, but the attenuation rate declines with the cycle numbers. In the meantime, there exists a sharp drop in capacity in the first 5 cycles but little change after 10 cycles for nickel disulfide cells. Therefore, the main factor influencing performance of Li-ion cells is the doping of iron elements, although the small particle size can do a great deal to improve its discharge capacity, it is at the cost of destroying the crystal structure and increasing internal stress due to lengthy ball milling (they are both adverse to cell performance improvement). In addition, the charge/discharge capacities were kept at 273, 273, 227 and 228 mAh g^{-1} even after 20 cycles for both Li/Fe-doped NiS_2 and Li/NiS_2 cells, which also indicates their high Coulombic efficiency of 100% and 99.6%, respectively.

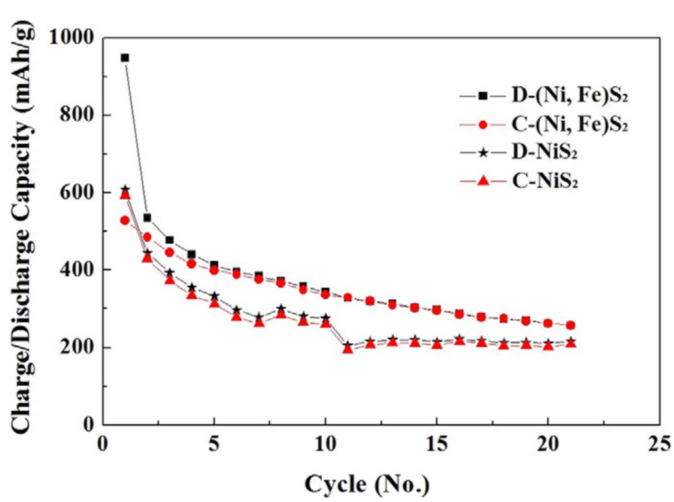

Fig. 11. Cycle performances of Li/NiS_2 and Li/Fe-doped NiS_2 cells prepared by PBM using wet milled particles at room temperature.

4. Conclusions

In this study, MA was successfully applied to synthesize fine NiS_2 and Fe-doped NiS_2 compounds by SM and further, BMM was applied to prepare each of the wet milled powders. Following this, the cathodes were separately manufactured, using SM and PBM for the dry milled powders and only PBM for the wet milled powders. The results show that SM can be of great help in improving the initial discharge capacity due to its better dispersibility, but displays relatively poor cycle properties mainly due to higher internal stress in the crystal structure. In addition, the wet milling process is helpful in decreasing particle size, increasing the specific surface area and further improving the performance of Li/Fe-doped NiS_2 cells prepared by PBM, however, it does not seem to apply to Li/NiS_2 cells as they show a lower capacity than dry milled cells. Overall in comparison, the main factor influencing the performance of Li-ion cells is the doping of iron elements, although the small particle size can help improve discharge capacity, but at the cost of destroying the crystal structure and increasing internal stress due to lengthy ball milling, which are both adverse to cell performance improvement. Therefore, further research on doping principles and methods in the future is very important.

Acknowledgements

This research was supported by Basic Science Research Program (2009-0071729) and WCU program (R32-20093) through the National Research Foundation of Korea (NRF) and Ministry of Education, Science and Technology.

References

[1] Y.P. Wu, H.P. Zhang, F. Wu, C.H. Li, Polymer Lithium Ion Batteries, Chemical Industry Press, Beijing, 2006, pp. 104–110.
[2] F. Wu, H.X. Yang, Green Secondary Batteries, Science Press, Beijing, 2009.
[3] A. Ennaoui, H. Tributsch, Iron disulfide solar cells, Journal of Solar Cells 13 (2) (1984) 197.
[4] P.R. Bonneau, P.K. Shibao, R.B. Kaner, Low-temperature precursor synthesis of crystalline nickel disulfide, Inorganic Chemistry 29 (13) (1990) 2511.
[5] J.C. Panigrahi, P.K. Panda, Transition-metal chalcogenide materials. Quick and convenient methods of synthesis of crystalline nickel (II) disulfide, Materials Letters 12 (1–2) (1991) 112.
[6] X.H. Chen, R. Fan, Low-temperature hydrothermal synthesis of transition metal dichalcogenides, Chemistry of Materials 13 (3) (2001) 802.
[7] X.F. Qian, Y.D. Li, X. Yi, Y.T. Qian, The synthesis and morphological control of nanocrystalline pyrite nickel disulfide and cobalt disulfide, Materials Chemistry and Physics 66 (1) (2000) 97.
[8] A. Olivas, I. Villalpando, S. Sepúlveda, O. Pérez, S. Fuentes, Synthesis and magnetic characterization of nanostructures N/WS_2, where N = Ni, Co and Fe, Materials Letters 61 (21) (2007) 4336.
[9] A. Ennaoui, S. Fiechter, W. Jaegermann, H. Tributsch, Photoelectrochemistty of highly quantum efficient single-crystalline FeS_2 (pyrite), Journal of the Electrochemical Society 133 (1) (1998) 353.
[10] M.R. Hilton, R. Bauer, S.V. Didziulis, M.T. Dugger, J.M. Keem, J. Scholhamer, Structural and tribological studies of MoS_2 solid lubricant films having tailored metal-multilayer nanostructures, Surface and Coatings Technology 53 (1) (1992) 13.
[11] F. Disma, L. Aymard, L. Dupont, J.M. Tarascon, Effect of mechanical grinding on the lithium intercalation process in graphites and soft carbons, Journal of the Electrochemical Society 143 (12) (1996) 3959.
[12] J.S. Kim, H.J. Ahn, H.S. Pyu, D.J. Kim, G.B. Cho, K.W. Kim, T.H. Nam, H.J. Ahn, The discharge properties of Na/Ni_3S_2 cell at ambient temperature, Journal of Power Sources 178 (2) (2008) 852.
[13] E. Strauss, D. Golodnitsky, E. Peled, Study of phase changes during 500 full cycles of Li/composite polymer electrolyte/FeS_2 battery, Electrochimica Acta 45 (8–9) (2000) 1519.